Available online at www.sciencedirect.com
ScienceDirect
Journal of Nuclear Materials 357 (2006) 138–146
journal of nuclear materials
www.elsevier.com/locate/jnucmat

Long-term erosion and re-deposition of carbon in the divertor region of JT-60U

Y. Gotoh [a], T. Tanabe [b,*], Y. Ishimoto [c], K. Masaki [c], T. Arai [c], H. Kubo [c], K. Tsuzuki [c], N. Miya [c]

[a] *Nihon Advanced Technology Co., Ltd., 3129-45 Hibara, Muramatsu, Tokai-Mura, Ibaraki-ken 311 0193, Japan*
[b] *Kyusyu University, Interdisciplinary Graduate School of Engineering Science, Department of Advanced Energy Engineering Science, 6-10-1, Hakozaki, Higashi-ku, Fukuoka 812 8581, Japan*
[c] *Japan Atomic Energy Agency, 801-1 Mukouyama, Naka-shi, Ibaraki-ken 311 0193, Japan*

Received 23 February 2006; accepted 2 June 2006

Abstract

Erosion and redeposition profiles of carbon tiles used in the W-shaped divertor of JT-60U with all carbon plasma facing wall are studied. The inner divertor is mostly covered by carbon redeposited layers, while the outer divertor mostly eroded. In the dome region, the erosion dominates on the inner dome-wing, while redeposited on the outer dome-wing. The redeposited layers on the outer dome-wing show very clear columnar structures indicating local carbon transport form the outer divertor to the outer dome-wing. The weight gain by the redeposition extrapolated to the whole divertor area is 0.55 kg. Since the extrapolated total erosion is about 0.33 kg, the remaining 0.22 kg must be originated from the main chamber erosion. Significant amount of the redeposition is caused locally by multiple processes of erosion, ionization and prompt redeposition toward inboard direction owing to gyration along magnetic filed line. This inboard transport is one of the reasons for small redeposition on the plasma shadowed area of the W shaped divertor of JT-60U with pumping slots placed at the bottoms side.

PACS: 52.40.Hf; 52.55.Fa

1. Introduction

Studies on erosion/redeposition at the plasma facing walls of fusion experimental devices are indispensable for elucidation and control of (1) impurity generation, transport and accumulation processes, (2) hydrogen isotope behaviors and long-term tritium inventories in a vacuum vessel and for (3) lifetime evaluation of divertor plates. In–out asymmetry in erosion/redeposition, i.e. the deposition domination on the inner divertor plate while the erosion on the outer divertor plate, has been commonly found in divertor tokamaks [1–3]. Large amount of carbon redeposition and hydrogen (tritium) incorporation in it were found on the plasma shadowed area of the inner divertor including louvers for cryo-pumps of Joint European Torus

* Corresponding author. Tel./fax: +81 92 642 3795.
E-mail address: tanabe@nucl.kyuhsu-u.ac.jp (T. Tanabe).

0022-3115/$ - see front matter © 2006 Elsevier B.V. All rights reserved.
doi:10.1016/j.jnucmat.2006.06.005

(JET), especially in the MkIIA divertor configuration [4]. In the MkIIA divertor configuration, divertor pumping ducts were set at the inboard side between the horizontal and vertical target tiles of the inner divertor with divertor strike points mostly on the vertical target tile. Different from JET, the divertor pumping in JT-60U is performed through the inner and the outer slots located in the private flux region at the bottom sides of the W shaped divertor. Consequently the erosion/redeposition characteristics of JT-60U are quite different from those of JET. The aim of the present study is to show poloidal profiles of the erosion/redeposition in the W-shaped divertor of JT-60U, especially focusing to those on the dome area (private flux region) and the outer pumping slot. From mass balance between the erosion and the redeposition, long term net erosion and redeposition in the W-shaped divertor region is also discussed.

Another focus is given to the detailed structure of the carbon deposited layers. Columnar structures were often found for the redeposited layers in tokamaks [5,6]. Orientation of the columnar axis may provide us information on an incident angle of incoming impurity carbon atoms on to the tile surface [7].

2. Experimental

In the present study, erosion and redeposition were investigated for carbon tiles used in the W-shaped divertor region of JT-60U in 1997–2002 experimental campaigns. In 1997–1998, about 5000 discharges were performed with the inner slot pumping (ISP), while in 1999–2002, about 9000 discharges were made with both the inner and the outer slots pumping (BSP). Fig. 1 shows the poloidal locations of analyzed tiles in the W-shaped divertor region. The total time of neutral beam injection (NBI) heating during the campaign was about 3×10^4 s. Most of the first wall tiles and the inner dome-wing tiles were made of isotropic graphite (ETP-10, Ibiden and IG-110U, Toyo-Tanso). Tiles for the divertor plate, the dome-top and the outer dome-wing were carbon fiber composite (CFC: CX-2002U). Operation temperature of the vacuum vessel was around 573 K. All carbon tiles were fixed to base plates on the vessel wall mechanically and only inertially cooled. During the discharges, therefore, plasma heat load raised bulk temperature of the tiles by 0–200 K depending on the location of the tiles, which was measured by thermocouple, embedded 6 mm beneath the tile surface.

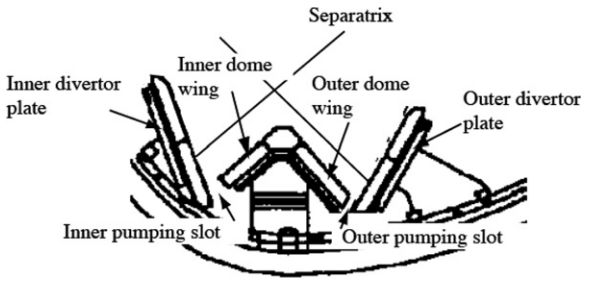

Fig. 1. Cross-sectional view of the W-shaped divertor region of JT-60U with pumping slots at both bottoms.

The net erosion depths and redeposition thicknesses on the divertor tiles were determined from tile thickness changes measured by a micrometer (surface profilometry). The precision of the profilometry was around 3 μm [3]. From the cross-sectional view of the tile including redeposited layers, the thickness of the redeposited layers and their sub-μm structures were observed by a scanning electron microscope (SEM: Hitachi type S-300 H). The cross-section of the tiles was prepared by fracturing the tiles in both the poloidal and toroidal directions assisted by slit notches of a 0.5 mm width formed at the rear faces. The SEM observations were made at a beam voltage of 5 kV. Thickness resolution for redeposited layers was estimated at 0.2 μm. The net erosion and redeposition thicknesses observed by the profilometry generally agree with those observed by SEM. However, the thin redeposition layers were sometimes observed on the erosion dominated area, resulting in small difference in the measurements of the profilometry and SEM.

3. Results

Fig. 2(b) shows poloidal thickness profiles of the redeposited layers on the inner divertor tiles, while Fig. 3(b) shows poloidal erosion depth profiles on the outer divertor tiles measured by the profilometry. The measurements were made along three different toroidal lines as indicated in Figs. 2(a) and 3(a). Each profile is very similar, indicating uniform redeposition and erosion in toroidal direction. The maximum deposition thickness was about 230 μm on the inner divertor tile, while the maximum erosion depth was 70–80 μm on the outer divertor tile. SEM cross-sectional views for the redeposited layers on the inner divertor tiles are shown in Fig. 2(d). The

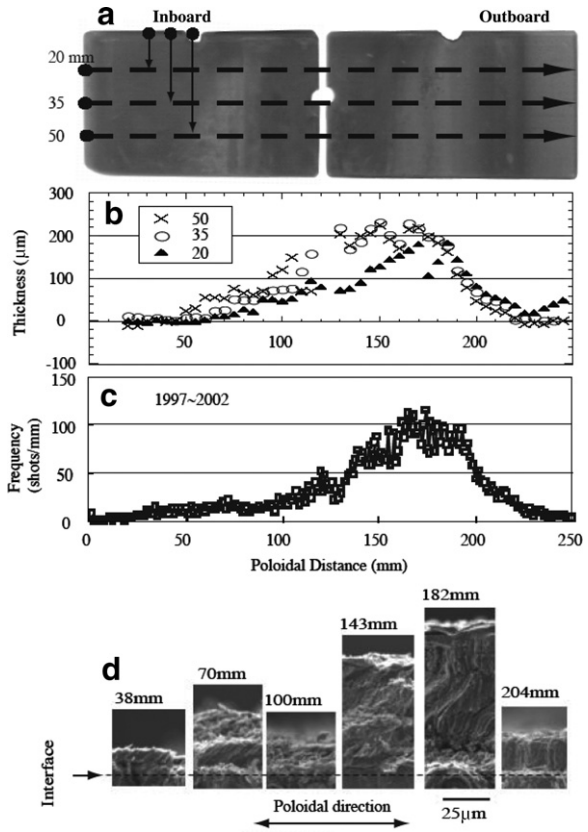

Fig. 2. (a) Photographs of two inner divertor tiles, (b) Poloidal thickness distribution of the redeposited layers, and (c) Poloidal frequency diagram of divertor-hit-points in the 1997–2002 experimental campaigns. Measurements were made along three different lines on the photograph shown in (a). SEM cross-sectional views for selecting points are shown in (d). The maximum thickness of around 230 μm was located at around 160 mm from the inboard end of the inner divertor tile.

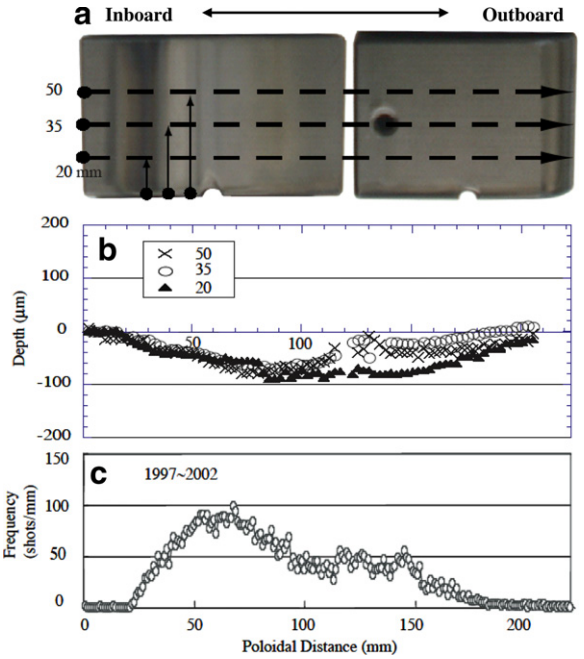

Fig. 3. (a) Photographs of two outer divertor tiles, (b) Poloidal distribution of the erosion depth, and (c) Poloidal frequency diagram of divertor-hit-points in the 1997–2002 experimental campaigns. Measurements were made along three different lines on the photograph shown in (a).

redeposited layers clearly show columnar structures with their axes declined from the surface normal. Frequency histograms of divertor-hit-points for the inner and the outer divertor tiles in 1999–2002 experimental campaigns are shown in Figs. 2(c) and 3(c), respectively. One can note that the poloidal distribution of the thickness of the redeposited layers on the inner divertor (Fig. 2(b)) is very similar to that of the divertor-hit-points distribution (Fig. 2(c)), though the former slightly shifted to the inboard side. The erosion maximum on the outer divertor (Fig. 3(b)) more clearly shifted to the outboard side from the most frequent divertor-hit-points (Fig. 3(c)). Both are indications of local carbon transport to the inboard side as discussed later.

It is important to note that the most of the outer divertor surface was net-eroded area, though SEM cross-sectional views indicated thin redeposited layers on some area. The most inboard side (left side) of the outer divertor tile was not net-eroded but covered by the redeposited layers of 3 μm in thickness. The inboard end side of the inner divertor tile was also covered by the redeposited layers of a few μm in thickness as shown in cross-sectional SEM imagers of Fig. 4(a)–(c), corresponding at 3.5 mm, 7.5 mm and 9.5 mm down from the front face to rear face, respectively.

Opposite to the divertor tiles, the inner dome-wing tile was mostly eroded and the outer dome-wing tile redeposited as seen in Figs. 5 and 6 where are shown three poloidal profiles of the erosion depth on the inner dome-wing tile and the thickness of the redeposited layers on the outer dome-wing tile. No redeposition was found on the inner dome-wing tile by the SEM observation. As shown in the Fig. 6, the outer dome-wing tile was covered by the redeposited layers and their thickness increased from the dome top to the bottom, showing sharp increase to the maximum thickness of 120 μm at the bottom edge.

The poloidal SEM cross-sectional views of the near bottom edge region of the outer dome-wing tile

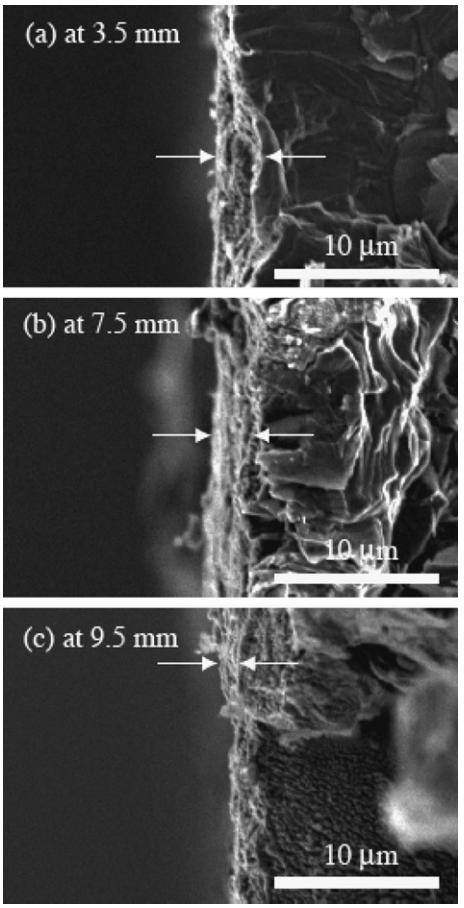

Fig. 4. Cross-sectional SEM images of the redeposited layers on the inboard end side of the inner divertor tile, where was not directly facing plasma. (a)–(c) were respectively taken at 3.5 mm, 7.5 mm and 9.5 mm down from the front face to the rear face. Arrows in the figures indicate the redeposited layers.

were shown in Fig. 7(a)–(c), near the bottom edge, the edge and the end side, respectively (see the inset of Fig. 7). The toroidal SEM cross-sectional image is given in Fig. 8. In both figures, the redeposited layers with columnar structure were appreciable and the directions of the axes were indicated by solid arrows in the figures. In Fig. 7, the directions of particle incidence were also indicated by dotted arrows, which will be discussed later. At the bottom end side of the outer dome-wing (see Fig. 7(c)), different from the other two facing plasma (Fig. 7(a) and (b)), the columnar axis declined downward from the surface normal. A toroidal cross-section of the redeposited layers near the bottom edge shown in Fig. 8 indicates a little inclination of the columnar structure with target normal (towards clockwise direction of the torus as indi-

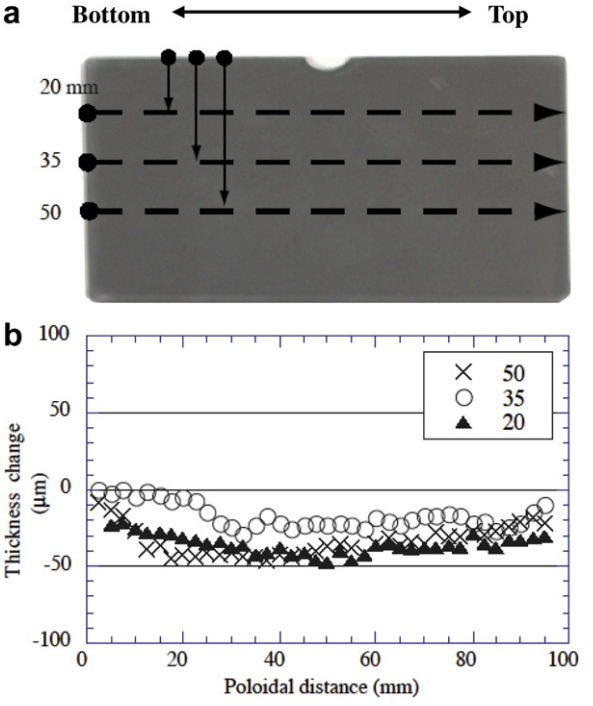

Fig. 5. (a) Photographs of the inner dome-wing tile and (b) poloidal distributions of the erosion depth. Measurement was made at three different lines on the photograph shown in (a).

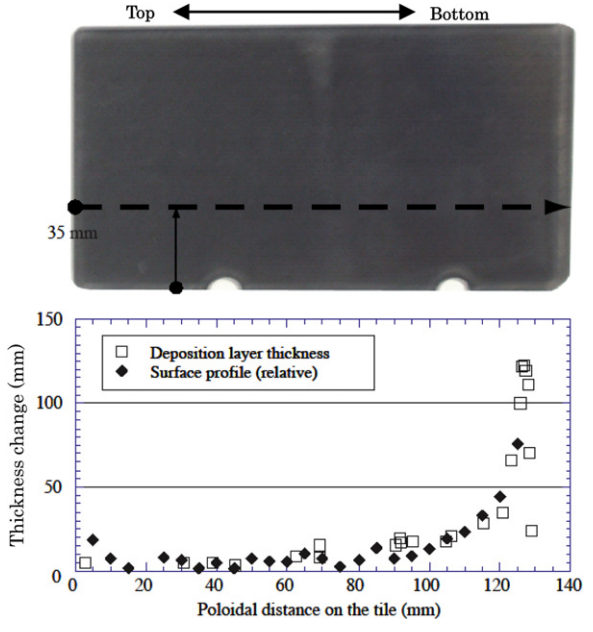

Fig. 6. Poloidal thickness distribution of the redeposited layers on the outer dome-wing tile. The net deposition determined by the surface profilometry was compared with the thickness determined by SEM cross-sectional images.

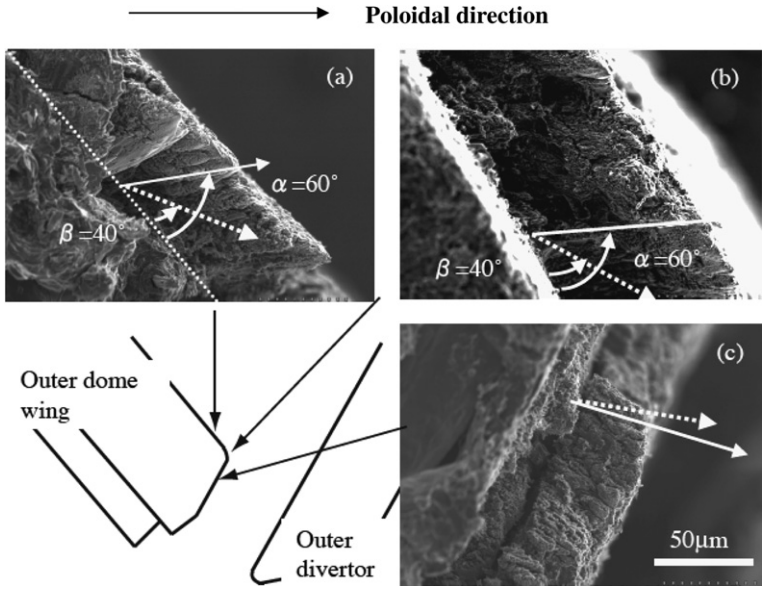

Fig. 7. SEM cross-sectional images of the redeposited layers at poloidal sections on the outer dome-wing tile: (a) at the front face, (b) on the outer edge, (c) at the outer end face. Arrows in solid line show direction of column growth. Arrows in dashed lines show incoming direction of adsorbed carbon atoms predicted by a 'tangent rule' (see text).

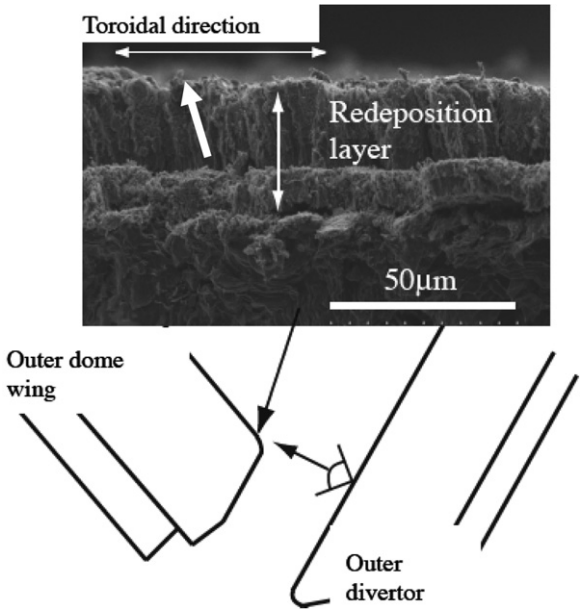

Fig. 8. SEM cross-sectional images of the redeposited layers at the front face of the outer dome-wing tile. The image was taken at a toroidal section of the redeposition layer.

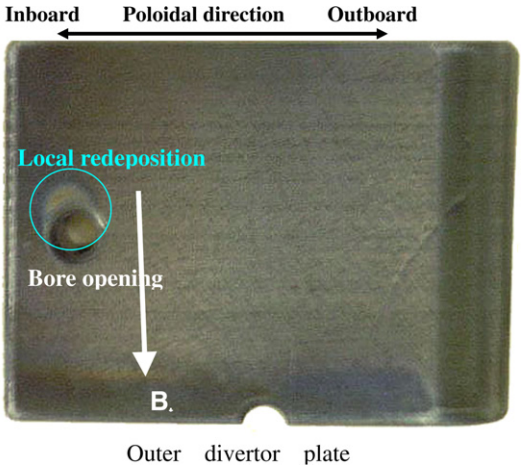

Fig. 9. Local redeposition near bore opening on the eroded inner divertor tile.

cated an arrow). The direction of the redeposition is more clearly seen in local redeposition near the bore opening of the outer divertor tile as shown in Fig. 9. Most of the surface of this outer divertor tile was eroded. The opposite side of the bore opening was eroded. One can see the redeposition directed a little inboard side along the magnetic filed line.

4. Discussion

4.1. Mass balance of carbon transport

Recently, volumetric density of the redeposited layers on the inner divertor tile has been measured [8] to be 910 kg/m^3, nearly a half of that of CFC

composite (CFRC: CX-2002U, 1700 kg/m^3). Assuming full toroidal symmetry as suggested by three different redeposition profiles in Fig. 2(b), the total amount of carbon erosion/redeposition in the divertor region was estimated. Increment of carbon by the redeposition was 0.36 kg for the inner divertor tiles, −0.09 kg by the erosion for the inner dome-wing, −0.25 kg for the outer divertor, and 0.18 kg for the outer dome-wing. The weight of the collected dust in the divertor region was measured to be 0.01 kg [9,10]. Adding all above, the net deposition of the divertor area of JT-60U was 0.21 kg, indicating about 40% [(0.36−0.21)/0.36] of the net deposition of the divertor area must originate from the first wall (main chamber).

According to this net deposition, carbon deposition rate in the divertor region can be estimated at 9×10^{20} C/s, divided by density of the redeposited layers 910 kg/m^3 and the integrated NBI heating time during 1997–2002 experimental campaigns. The value is a little higher than 3×10^{20} atoms/s previously determined for the inner side pumping geometry [7], probably because of the higher NBI power for the both sides pumping period. Thus carbon redeposition in the divertor region would reach 560 kg/year, if the high NBI power discharges were continuously made. Since around 40% of the net deposition on the divertor was attributed to the erosion of the first wall, the net erosion of the first wall for one year high power operation would end up with about 220 kg/year. This number is about 1/4 of that estimated for JET-MkIIA divertor (1000 kg/year) [11].

4.2. Erosion and deposition mechanism

In–out asymmetry in erosion/redeposition, i.e. redeposition on the inner divertor tile while erosion on the outboard divertor tile, was commonly observed on divertor tiles of large tokamaks [1–4]. Higher plasma temperature of the outer divertor is likely the cause of the erosion, while colder and denser plasma at the inner divertor causes redeposition of carbon. The eroded carbon at the outer divertor would be transported to the inner divertor along SOL flows towards the inner divertor at the low-filed-side midplane observed by Mach probes [11]. The $E_r \times B$ drift flow from the outer divertor to the inner divertor through the private region could also cause carbon transport [12,13]. However, as discussed above, the mass balance of carbon eroded at the outer divertor and redeposited at the inner divertor is missing and the erosion at the first wall must be additional source for the redeposition on the inner divertor, of which mechanism is still not clear.

In addition to this in–out asymmetry, the present study shows another asymmetry at the dome area, i.e., opposite to the divertor plates, the erosion on the inner dome-wing and the deposition on the outer dome-wing. Furthermore the outboard edge of the inner divertor was not redeposited, whereas the inboard edge of the outer divertor was rather covered by the redeposited layers, though the both edges were shadowed from plasma.

All these observations strongly suggest the inboard local transport of carbon impurities, which could be an additional carbon transport mechanism through private flux region. According to recent tritium profiling on the tile sides [14–16], the carbon redeposition on the sides of tiles at erode area was appreciable. As already show in Fig. 9, the local erosion and redeposition near a bore opening was clearly observed on the eroded tile of the outer divertor. This confirms short range carbon transport, i.e. eroded carbon neutrals were spontaneously ionized and gyrated along magnetic filed lines to be redeposited near starting surface, 'prompt redeposition' as already confirmed by high Z materials [17]. Multiple process of erosion and redeposition results in net carbon inboard transport owing to normal magnetic field configuration [18].

In the present work, the redeposition pattern observed on the outer dome-wing by SEM (see Figs. 6 and 7) gave further confirmation of the local inboard transport as discussed below. It is widely known that in plasma assisted carbon deposition processes, columnar structure is formed when an incident angle of impinging species is not a surface normal of the substrate but has a glancing angle at relatively low temperatures and an empirical role between an inclination angle α of the columnar structure and an incident angle β of the deposition species called a tangent rule [19,20],

$$\tan\alpha = 2\tan\beta,$$

is well established. As already reported [7], the redeposited layers on the open divertor of JT-60 showed columnar structures obeying the tangent rule. According to this equation, with the inclination angle α (60°) given in solid arrows in Fig. 7(a) and (b), the impinging angles relative to the substrate surface, β, of the deposition species were calculated to be 40° as shown with dotted arrows. The impinging angles of the plasma facing surface (Fig. 7(a)

and (b)) were also calculated to be around 30–70° by the magnetic filed line according to [21], which nearly agrees with 40° determined by the tangent rule. Furthermore, the inclination of the columns towards the clockwise direction of the torus (Fig. 9) indicated that carbon species impinged on to the dome-wing tile somewhat in the counter clock-wise direction agreeing with the fact that incoming direction of ions at the outer divertor plate is usually counter clock-wise direction of the torus. The direction of the prompt redeposition is more clearly seen in Fig. 9, a little inboard side along the magnetic filed line.

Therefore, the redeposited layers around the outer edge of the outer dome-wing are concluded to be formed due to the redeposition of the carbon species eroded from the front surface of the outer divertor plate. The bottom side of the dome was not facing plasma and the particles seem to come directly from the outer divertor without ionization and gyration.

Since ionized carbon and hydrocarbons produced near eroded surface might not be allowed to directly travel from the outer divertor to the outer dome-wing through the divertor plasma, the charge exchange neutral should have contributed to the deposition according to this mechanism. Then the following question remains. Taking rather high density of the divertor plasma into account, even charge exchange neutrals must collide to another neutrals, electrons and ions, and hence carbon impurities released by the erosion of the outer divertor do not likely travel directly to the outer dome-wing. In other words, why the incident particle to the outer dome-wing to make columnar structure could keep the momentum parallel to the incident angle β. In case if the eroded particles (mostly as neutrals) were emitted with the cosine distribution and a little higher energy than plasma temperature, like physically sputtered particles, they could keep their initial momentum to the inward direction from the outer divertor surface. Actually the poloidal thickness profile of the redeposited layers on the plasma facing surface of the outer dome-wing tile is well represented to the solid angle, $\sin\gamma/L^2$, where L the distance from the outer divertor and γ declining angle of the outer dome-wing and the outer divertor tile, as shown in Fig. 10. This means that carbon impurities originated from the outer divertor tile directly traveled to the outer dome-wing, and neutrals in the divertor plasma did not shadow or hinder the movement of the carbon impurities.

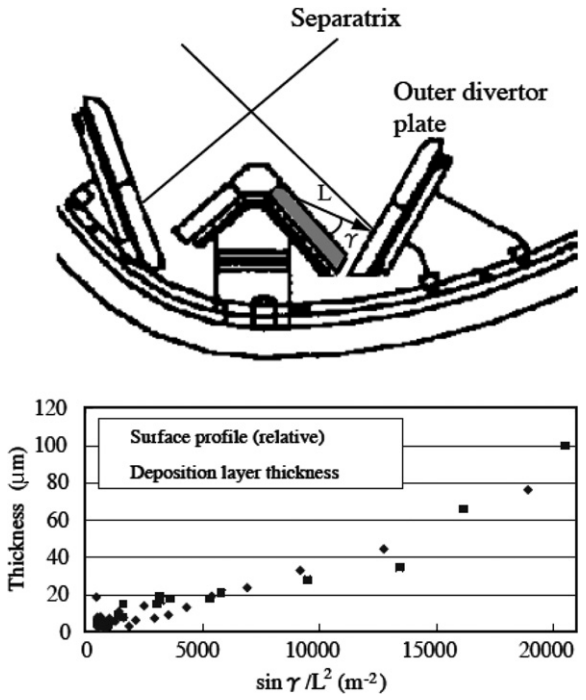

Fig. 10. Dependence of the thickness of the redeposited layers of the outer dome-wing on a solid angle from the outer divertor ($\sin\gamma/L^2$) (see text).

For the same reason, the carbon inboard transport on the inner dome-wing did not cause the redeposition, but the eroded species were transformed to the direction of the inner divertor. Still it is not clear why the inner dome-wing was not redeposited by impinging carbon from plasma directly.

As already noted that the redeposition profile on the inner diver was shifted to the inboard side a little from the divertor-hit-points profile (see Fig. 2) and the near bottom edge the outer divertor was slightly redeposited. All those results make us to conclude that carbon is dominantly transported toward the inboard side from the divertor-hit-point.

4.3. Comparison of JT-60U W-shaped divertor and JET MkIIA divertor

As already mentioned the net deposition and hence erosion was found to be much less in JT-60U compared to JET. Here we discuss the cause of the difference. Of course both machines were operated with different plasma characters, which could cause such difference. Nevertheless, at least the redeposition rate at the plasma facing redeposited area seems similar [22], requesting other cause than the difference of the plasma character.

Since the pumping slots were set at the bottom in the W-shaped JT-60U divertor, different from the JET MKIIA divertor, the inboard carbon transport hinders the hydrocarbon exhaust to the pumping slot at the bottom (see Fig. 1). Actually near the bottom edge on the inner divertor was hardly covered by the redeposited layers, as shown in Fig. 2, while the most inner side edge of horizontal target tile of the JET MkIIA divertor used in DTE1 campaign heavily redeposited, and almost no redeposition was found in the inner slot shadowed zone in JT-60U. The inboard carbon transport discussed above was also evidenced by the redeposition on the bottom side surface of the outer divertor tile facing to the pumping slot in JT-60U (not shown here).

Thus, divertor geometry such that pumping ducts are placed at the bottom of the W-shaped divertor, is likely effective in suppressing carbon deposition in the inner pumping slot. On the other hand, appreciable carbon deposition observed on the outer dome-wing remains a concern. Significant tritium retention owing to carbon deposition was also observed in the horizontal target tile of the outer divertor in JET MkIIA divertor [23].

Temperature of tile surfaces is also an important factor. The significant carbon deposition in JET was mostly observed at plasma shadowed area in the pumping slot at the inner divertor, probably assisted by the inboard carbon transport. The temperature of that area might not rise without plasma heat load; even JET was operated at similar temperature as JT-60U. On the other hand, the temperatures of most of the redeposited area of the JT-60U divertor tiles are very likely well above 700 K during discharges. However, the dome area particularly the bottom of the dome tiles would remain lower temperature which could enhance the carbon deposition. The carbon redeposition at higher temperature incorporate less hydrogen and more strongly stuck the substrate. Accordingly, much less dust was collected in JT-60U compared to JET [10].

Another difference is the tile alignment. Divertor tiles of JT-60 were toroidally well aligned having almost no steps between the toroidally neighboring tiles. As a result, both redeposition and erosion profiles were toroidally uniform as shown in Figs. 2, 3, and 6. In JET MkIIA divertor, toroidally a few mm step between divertor tiles was made in order to avoid the edge heating effect. Accordingly toroidal deposition profiles given by tritium retention profiles were nonuniform, having less redeposition at the inner divertor or larger erosion at the outer divertor at the one tile side nearer to plasma and vise verse at the other tile side [23]. Thus toroidal fine alignment of the tiles could reduce the erosion and result in less carbon redeposition in JT-60U.

5. Conclusion

In–out asymmetry in erosion/redeposition pattern was confirmed at the inner and the outer divertor tiles used in the W-shaped JT-60U during the experimental campaign from 1997 to 2002; erosion dominates the outer divertor tiles with the maximum erosion depth of 70 μm, whereas redeposition dominates the inner divertor tiles with maximum thickness of 230 μm. The poloidal distribution of the thickness of the redeposited layers on the inner divertor tiles was very similar to that of the divertor-hit-points distribution, though the former slightly shifted to the inboard side. The erosion maximum on the outer divertor clearly shifted to the outboard side from the most frequent divertor-hit-point.

In the dome area, the opposite in–out asymmetry appeared. The inner dome was mostly eroded, while the outer dome wing tile was covered by the redeposited layers with their thickness increasing from the dome top to the bottom end of the maximum thickness of 120 μm. The redeposited layers show columnar structures. In the toroidal direction, the axes of the columns incline towards the clock-wise direction of the torus, while poloidally towards the outer divertor side. Poloidal and toroidal distributions of the thicknesses and orientations of the columns indicate that the observed redeposition on the outer dome-wing is caused by transport of carbon atoms eroded at the outer divertor tile. The inner dome-wing is mostly eroded. All these observations indicate that local carbon transport toward the inboard side plays an important role on the carbon redeposition processes.

Long-term net deposition of carbon in the divertor region is 0.55 kg. About 60% of the net deposition originates from the erosion in the divertor area, while remaining 40% should be attributed to the erosion at the first wall (main chamber). The net deposition is much smaller than JET, probably owing to fine tile alignment, higher surface temperature, and divertor structure avoiding carbon transport to plasma shadowed area.

Acknowledgements

The authors gratefully thank to Drs N. Asakura and T. Nakano for fruitful discussions. This work was partly supported by Grand-in-Aid of Ministry of Education, Culture, Sports, Science and Technology of Japan (No. 17206092).

References

[1] D.G. Whyte, J.P. Coad, P. Franzen, H. Maier, Nucl. Fusion 39 (1999) 1025.
[2] J.P. Coad, P.L. Andrew, A.T. Peacock, Phys. Scripta T81 (1999) 7.
[3] Y. Gotoh, J. Yagyu, K. Masak, et al., J. Nucl. Mater. 313–316 (2003) 370.
[4] J.P. Coad, N. Bekris, J.D. Elder, et al., J. Nucl. Mater. 290–293 (2001) 224.
[5] J. von Seggern et al., Phys. Scripta T81 (1999) 31.
[6] R. Reichle, D. Guilhem, R. Mitteau, et al., Nucl. Fusion 43 (2003) 797.
[7] Y. Gotoh, T. Arai, J. Yagyu, et al., J. Nucl. Mater. 329–333 (2004) 840.
[8] Y. Ishimoto, Y. Gotoh, T. Arai, et al., J. Nucl. Mater. 350 (2006) 301.
[9] K. Masaki, K. Sugiyama, T. Hayashi, et al., J. Nucl. Mater. 337–339 (2005) 553.
[10] J. Phillip Sharpe, P.W. Humrickhouse, C.H. Skinner, et al., J. Nucl. Mater. 337–339 (2005) 1000.
[11] G.F. Matthews, J. Nucl. Mater. 337–339 (2005) 1.
[12] Y. Ishimoto, Y. Gotoh, T. Arai, et al., Proc. 12th ICFRM, J. Nucl. Mater., to be published.
[13] N. Asakura, H. Takenaga, S. Sakurai, et al., Nucl. Fusion 44 (2004) 503.
[14] T. Tanabe, K. Sugiyama, C.H. Skinner, et al., Fusion Sci. Technol. 48 (2005) 577.
[15] T. Tanabe, K. Sugiyama, C.H. Skinner, et al., J. Nucl. Mater. 345 (2005) 9.
[16] K. Sugiyama, T. Tanabe, K. Masaki, N. Miya, Proc. 12th ICFRM, J. Nucl. Mater., to be published.
[17] Y. Ueda, T. Tanabe, V. Philipps, et al., J. Nucl. Mater. 220–222 (1995) 240.
[18] K. Ohya, T. Tanabe, J. Kawata, Fusion Eng. Design 81 (2006) 205.
[19] P. Ramanlal, L. Sander, Phys. Rev. Lett. 54 (1985) 1828.
[20] R. Messier, J. Vac. Sci. Technol. A18 (2000) 1538.
[21] M. Shimada, T. Ohkawa, J. Nucl. Mater. 266–269 (1999) 906.
[22] T. Tanabe, Fusion Eng. Design 81 (2006) 139.
[23] T. Tanabe, N. Bekris, P. Coad, et al., J. Nucl. Mater. 313–316 (2003) 47.